RSC Advances

Highly Robust Tetrazolate Based Complexes for Efficient and Long-term Stable Dye Sensitized Solar Cells

Tharallah A. Shoker, Ralph Tanios, Remi Fayyad and Tarek H. Ghaddar*
Department of Chemistry, American University of Beirut, Beirut 11-0236, Lebanon

Abstract

We report on a new family of ruthenium poly-pyridyl complexes that bears tetrazolate based ligands (either bi-chelate as in T162 or tri-chelate as in T120 and T147), along with their spectroscopical, electrochemical, and theoretical characterization. Dye-sensitized solar cells (DSSCs) with these complexes show good conversion efficiencies that are highly dependent on the respective electrolyte composition especially in the case of T120 and T147, due to low lying LUMO's when compared to N719 and T162. DSSCs based on these dyes showed superb stability under light soaking at 70 ^{o}C for 2000 h. The T120 and T147 based cells retained their initial efficiencies after the long term-stability test, while the T162 and N719 efficiencies decreased by 18% and 40%, respectively.

Keywords: Impedance spectroscopy, Dye Sensitized Solar Cell, Ruthenium, Tetrazolate

* To whom correspondence should be addressed. Email: tarek.ghaddar@aub.edu.lb

Introduction

The dye sensitized solar cell (DSSC) is an ecofriendly and low cost solar energy to clean electricity device, which makes it a good candidate for commercialization.[1] Liquid electrolyte based DSSCs have reached more than 13% efficiencies for small area cells under AM 1.5 sunlight irradiation.[2, 3] However, there are some challenges that are still facing the DSSC field that render its commercialization difficult. Two of these challenges are the long term stability of the DSSC device under normal operating conditions, and the inadequate light harvesting ability of the DSSC in the near-IR region (> 800 nm) that results in efficiencies on the low side (lower than 15%).

The dye (an organic or inorganic sensitizer) is a key component in a DSSC. The well-known N719 dye, $(TBA)_2[(dcbpy)_2Ru(NCS)_2]$ (TBA = tetrabutylammonium and dcbpy = 4,4'-dicarboxy-2,2'-bipyridine),[4] has been for a long time one of the best performing sensitizers. Many research groups have been working on the molecular engineering of dyes in order to address the long-term stability and the near-IR absorption ability of such dyes. Designing metal based dyes that lack the thiocyanate ligand (SCN⁻), which is considered from long-term chemical stability tests as the weakest part in most ruthenium-based dyes,[5-7] is of great interest. In addition, red-shifting the absorption band of the sensitizer and increasing the molar absorption extinction coefficient in the visible and near-IR region may have positive effects on the DSSCs' efficiencies. Recently, a new class of ruthenium complexes that lack the SCN⁻ ligand and have better light harvesting properties than N719 has been introduced by different research groups.[8-18] The high interest in this class of ruthenium based dyes is due to their extended absorption in the visible region (down to 800 nm). Nevertheless, there are very few reports on the effect of using thiocyanate free dyes on the long-term stability of the DSSC.[19, 20]

Recently, we reported a new class of Ru^{II} dyes that bear either a bis- or tris-tetrazolate mono-dentate ligands that showed good DSSC performance.[8] However, the ancillary ligands were of the mono-dentate type that could be not advantageous for the long-term stability of DSSCs. Ruthenium complexes baring monodentate ligands are known to be prone to photo-substitution of the latter.[21, 22] Moreover, exchanging mono-dentate and even bi-dentate ligands to their tri-dentate analogs in ruthenium poly-pyridyl complexes usually results in an increase in the absorption extinction coefficient and a slight red shift of the ^1MLCT absorption band, as is the case for $Ru(bpy)_2(py)_2^{+2},$[23] $Ru(bpy)_3^{+2},$[24] and $Ru(trpy)_2^{+2},$[25] where py = pyridine, bpy = 2,2'-bipyridine and trpy = 2,2',2''-terpyridine. In the present study, we report the design and long-term stability tests of DSSCs incorporating three Ru^{II} based dyes, **T120**, **T147** and **T162**, that bear tridentate or bidentate ligands, based on tetrazolate moieties on the ancillary ligand, Scheme 1. The motivation behind the design of such dyes with multi-dentate ancillary ligands was the aim of increasing the optical absorptivity in the visible and near-IR that might boost the short-circuit photocurrent (J_{sc}) and thus the overall efficiency ($\%\eta$), and to increase the robustness of such dyes when subjected to prolonged thermal and light stress.
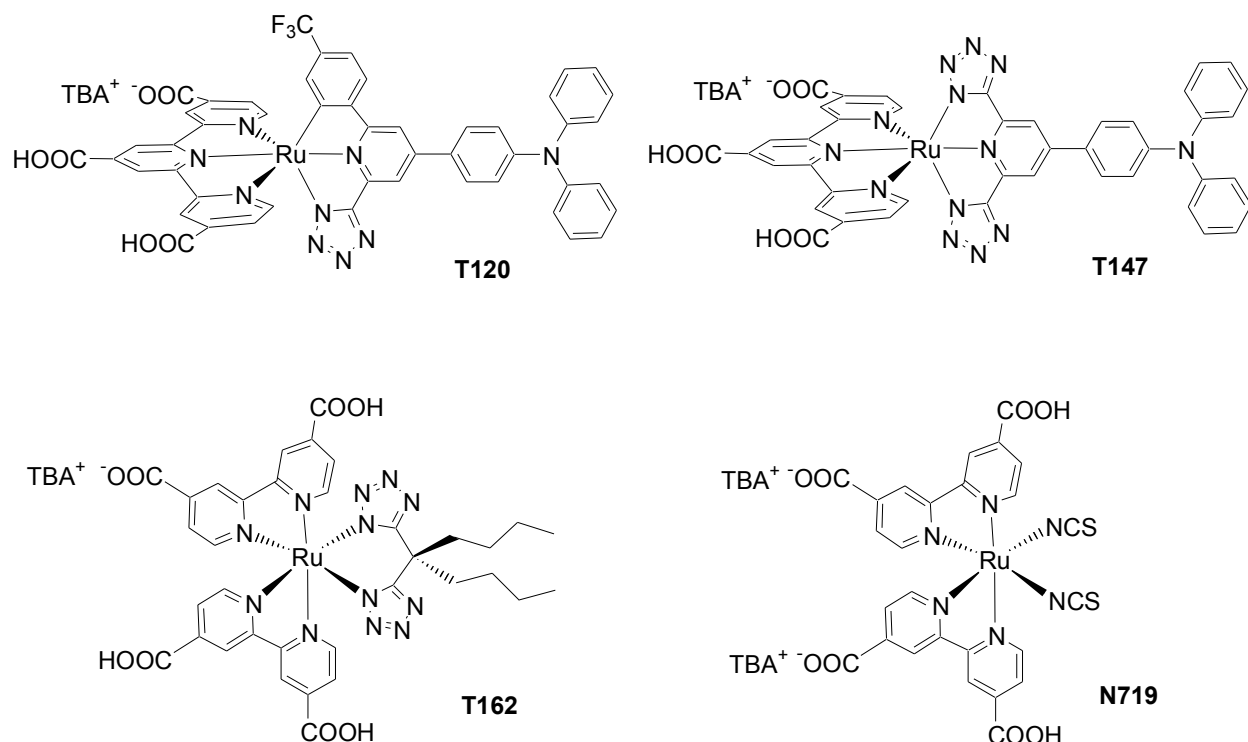
Scheme 1: Structures of the Ru^{II} sensitizers **T120**, **T147**, **T162** and **N719** (TBA$^+$ is tetrabutyl ammonium).

Experimental

Materials and Instrumentation. All organic chemicals were purchased from Sigma-Aldrich and used as supplied. The N719 dye was purchased from Solaronix (Switzerland). FTO glass "Tec15" and 'Tec8" were purchased from Pilkington (USA). TiO$_2$ colloids were purchased from Dyesol (Australia). 1-(2-oxo-2-(4-(trifluoromethyl)phenyl)ethyl)pyridinium iodide,[26] 2,2-dibutylmalanonitrile,[27] 4-chloro-2,6-dicyanopyridince,[28] (dcbpy)$_2$RuCl$_2$[29] and (4,4',4"-trimethoxycarbonyl-2,2':6',2"-terpyridine)RuCl$_3$[30] were prepared according to reported procedures in the literature. The NMR spectra (^{1}H and ^{13}C) were measured on a Bruker AM 500 MHz spectrometer. UV-vis spectra were recorded on a Jasco V-570 UV/vis/NIR. Steady state emission spectra were measured on a JobinYvon Horiba Fluorolog-3 spectrofluorometer. The electrochemical setup consisted of a three-electrode cell, with a stained TiO$_2$ film on FTO with the respective dye as the working electrode, a Pt wire ~ 1 mm diameter as the counter electrode, and Ag/Ag$^+$ (10 mM AgNO$_3$) as the reference electrode. The electrochemical mesearments were performed in 0.1 LiClO$_4$ in acetonitrile, and Fc/Fc$^+$ standard (0.63 vs NHE in acetonitrile) was used as a reference. Electrochemical impedance spectra of the DSSCs were performed with CH Instruments 760B (USA). The obtained impedance spectra were fitted with the Z-view software (v2.8b, Scribner Associates Inc.), and the reported fitted parameters are

within a 2% error. The spectra were performed at a forward bias voltage (between -0.5 and -0.8 V) in the frequency range 0.1 Hz - 10^5 Hz with oscillation potential amplitudes of 10 mV at RT under open circuit conditions at different light levels. IPCE% spectra were recorded using a Newport 74000 Cornerstone™ monochromator and a solar simulator illuminated by a Xenon arc lamp (Oriel) through an AM1.5 simulation filter (ScienceTech). Photocurrent vs. Voltage characteristics were measured with a Keithley 2400 sourcemeter. The irradiated area of the cell was 0.126 cm^2. Long-term stability measurements were performed at 70 ^{o}C and around 1 sun irradiation from a high-power tungsten lamp.

Computational Methods. Calculations were carried out using *Gaussian 03*.[31] Geometries were optimized using the 6-31G* basis set with (B3LYP), together with the Los Alamos effective core potential LanL2DZ[32] in water (C-PCM algorithm).[33] TD-DFT calculations were performed using the C-PCM with water as the solvent. Fifty singlet excited states were determined from the optimized structures.

Solar Cell Fabrication. Dye sensitized solar cells were fabricated using standard procedures. The TiO_2 films were made from colloidal solutions using the doctor blading method (2x times) on "Tec15" and then heated to 480 ^{o}C for 30 mins. This afforded a 12 μm thick TiO_2 film, on top of which a 6 μm TiO_2 scattering layer (300 nm TiO_2 particles) was deposited and reheated at 480 ^{o}C for 30 mins. A $TiCl_4$ post-treatment was applied to the films following reported procedures in the literature.[34] These films were then reheated at 480 ^{o}C for 30 min. The TiO_2 films were stained by the respective dye solution (0.3 mM) in 1:1 *t*-butanol:acetonitrile for 18 h. The counter electrodes were fabricated by applying a 2-3 μl/cm^2 of 5 mM H_2PtCl_6 in 2-propanol to the "Tec8" FTO glass, followed by heating in an oven at 400 ^{o}C for 20 minutes. Cell assembly was performed by sealing the counter electrode to the TiO_2 electrode with a 60 μm Surlyn (Dupont) spacer at ~ 100 ^{o}C for 3 mins. The corresponding electrolyte was introduced through two small holes, previously drilled through the counter electrode, which were then sealed with Surlyn.

CAUTION! Tetrazoles are highly energetic compounds with sensitivity towards heat and impact. Although we had no problems during the synthesis, proper protective measures should be used when undertaking work involving these compounds.

Preparation of 4-(4-diphenylamino-phenyl)-1,1-dimethoxy-but-3-en-2-one: To a solution of 4-(*N,N*-diphenylamino)benzaldehyde (10.44 g, 28 mmol) in ethanol (100 ml), 1,1-dimethoxypropan-2-one (5.90 g, 50 mmol) was added followed by piperidine (5.50 g, 50 mmol). The mixture was then heated to reflux for 48 h. After cooling, the solvent was removed in vacuo and the residue was extracted with chloroform (3x100 ml), dried over magnesium sulfate and the solvent was evaporated under reduced pressure. Purification was accomplished via silica gel column chromatography using hexane : ethyl acetate (5%) as the eluent to yield a pure yellow

solid (90% yield). ^{1}H NMR (300 MHz, CDCl$_3$): δ = 7.78 – 7.72 (d, J = 15.9 Hz, 1H), 7.46 – 7.43 (d, J = 8.7 Hz, 2H), 7.33 – 7.26 (m, 5H), 7.14 – 7.11 (m, 6H), 7.00 – 6.98 (d, J = 8.7, 2H), 6.95 – 6.89 (d, J = 15.8 Hz, 1H), 4.76 (s, 1H), 3.44 (s, 6H). ^{13}C NMR (75 MHz, CDCl$_3$): δ= 193.71, 150.46, 146.71, 144.96, 130.03, 129.41, 127.26, 125.57, 124.25, 121.26, 117.93, 103.60, 54.27. APPI MS (*m/z*): calculated for C$_{24}$H$_{24}$NO$_3$ [M + H]$^+$, 374.2; found, 374.0.

Preparation of 4-(4-diphenylamino-phenyl)-6-(4-trifluoromethyl-phenyl)-pyridine-2-carbaldehyde: A mixture of 4-(4-diphenylamino-phenyl)-1,1-dimethoxy-but-3-en-2-one (1.15 g, 3.1 mmol), 1-(2-oxo-2-(4-(trifluoromethyl)phenyl)ethyl)pyridinium iodide (1.21 g, 3.10 mmol) and ammonium acetate (2.5 g, excess) in ethanol (40 ml) was refluxed for 24 h. After cooling to room temperature, the solvent was evaporated under vacuo. The residue was extracted with chloroform (3x100 ml), dried over magnesium sulfate and the solvent was evaporated under reduced pressure. Without any further purification, the crude product was added to a mixture of CHCl$_3$ (15 mL), acetone (15 mL), distilled water (3.5 mL) and concentrated HCl (1.5 mL). The mixture was heated to reflux for 12 h. The resulting red solution was cooled to room temperature, extracted with chloroform (3x100 ml), dried over magnesium sulfate and the solvent was evaporated under reduced pressure. Purification was accomplished via silica gel column chromatography using hexane : ethyl acetate (10%) as eluent to yield the final product as a pure yellow solid (70% yield). ^{1}H NMR (300 MHz, CDCl$_3$): δ = 10.21 (s, 1H), 8.26 – 8.24 (d, J = 8.1 Hz, 2H), 8.15 – 8.13 (m, 2H), 7.80 – 7.78 (d, J = 8.1 Hz, 2H), 7.65 – 7.60 (m, 2H), 7.35 – 7.29 (m, 4H), 7.18 – 7.08 (m, 8H). ^{13}C NMR (75 MHz, CDCl$_3$): δ = 193.73, 156.85, 153.25, 150.37, 149.74, 146.96, 141.62, 131.66, 131.23, 129.55, 129.39, 127.90, 127.50, 125.93, 125.28, 124.02, 122.44, 121.79, 117.76. APPI MS (*m/z*): calculated for C$_{31}$H$_{21}$F$_3$N$_2$O [M + H$^+$]$^+$, 495.2; found, 495.0.

Preparation of 4-[4-(diphenylamino)phenyl]-6-[4-(trifluoromethyl)phenyl]picolinonitrile: A mixture of 4-(4-diphenylamino-phenyl)-6-(4-trifluoromethyl-phenyl)-pyridine-2-carbaldehyde (0.7 g, 1.4 mmol) and hydroxylamine hydrochloride (0.1 g, 1.4 mmol) was dissolved in ethanol (50 mL) and the mixture was heated at reflux for 2 h. After cooling, the solvent was evaporated under vacuo. The residue was extracted with chloroform (3x100 ml), dried over magnesium sulfate and the solvent was evaporated under reduced pressure to yield the crude oxime. Without any further purification, the oxime was dissolved in CH$_2$Cl$_2$ (10 mL) to form solution 1. In another round bottom flask (100 mL) CH$_2$Cl$_2$ solution of Ph$_3$P (0.34 g, 1.3 mmol) was treated with trifluoroacetic anhydride (0.31 g, 1.5 mmol) to form solution 2. Solution 2 was stirred for 10 min followed by the addition of solution 1 and triethylamine (0.16 g, 1.5 mmol). After stirring the mixture for 10 min, it was diluted with CH$_2$Cl$_2$ (20 ml) and washed with H$_2$O (30 mL) and brine (20 mL). The organic layer was dried over magnesium sulfate and the solvent was evaporated under reduced pressure. Purification was accomplished via silica gel column chromatography using hexane : dichloromethane (30%) as eluent to afford the product as a pure yellow solid (83% yield). ^{1}H NMR (300 MHz, CDCl$_3$): δ = 8.19 – 8.17 (d, J = 8.1 Hz, 2H), 8.09 – 8.08 (d, J = 1.8 Hz, 1H), 7.84 – 7.83 (d, J = 1.8 Hz, 1H), 7.78 – 7.75 (d, J = 8.4 Hz, 2H), 7.57

– 7.52 (m, 2H), 7.35 – 7.29 (m, 4H), 7.18 – 7.10 (m, 8H). ^{13}C NMR (75 MHz, CDCl$_3$): δ = 157.76, 150.37, 150.12, 146.78, 140.87, 134.47, 129.60, 128.09, 127.78, 127.48, 125.93, 125.88, 125.83, 125.44, 124.68, 124.25, 122.16, 120.65, 117.51. APPI MS (*m/z*): calculated for C$_{31}$H$_{21}$F$_3$N$_3$ [M + H]$^+$, 492.2; found, 492.2.

Preparation of: 4-{2-(1*H*-tetrazol-5-yl)-6-[4-(trifluoromethyl)phenyl]pyridin-4-yl}-*N,N*-diphenylbenzenamine: To a solution of 4-[4-(diphenylamino)phenyl]-6-[4-(trifluoromethyl)phenyl]picolinonitrile (0.5 g, 1.0 mmol) in DMF (100 mL), sodium azide (0.1 g, 1.5mmol) and ammonium chloride (80 mg, 1.5 mmol) were added. After stirring the reaction mixture at 120 °C for 3 h, it was cooled to RT and then poured into water and extracted with ethyl acetate (30 ml x 3). The organic layer was washed with brine, dried over MgSO$_4$, filtered and concentrated in vacuo. Purification was accomplished via silica gel column chromatography using hexane : ethyl acetate (20 %) as eluent to afford the final product as a pure yellow solid (85% yield). ^{1}H NMR (300 MHz, CDCl$_3$): δ 8.55-8.54 (d, 1H, *J* = 1.5 Hz), 8.23-8.21 (d, 2H, *J* = 8.1 Hz), 8.05-8.03 (m, 2H), 7.77-7.74 (d, 2H, *J* = 8.4 Hz), 7.67-7.64 (d, 2H, *J* = 9 Hz),7.35-7.30 (m, 2H), 7.19-7,10 (m, 8H). ^{13}C NMR (75 MHz, CDCl$_3$): δ 162.89, 156.87, 155.04, 149.82, 146.94, 144.17, 141.78, 129.55, 129.14, 127.88, 127.54, 125.80, 125.75, 125.32, 124.04, 122.35, 119.91, 119.19. APPI MS (*m/z*): calculated for C$_{31}$H$_{20}$F$_3$N$_6$ [M - H$^+$]$^-$, 533.2; found, 533.2.

Preparation of 4-(4-diphenylamino-phenyl)-pyridine-2,6-dicarbonitrile: To a round-bottom flask, 4-chloropyridine-2,6-dicarbonitrile (1.00 g, 6.17 mmol), 4-(diphenylamino)phenylboronic acid (2.24 g, 7.77 mmol), Pd(AcO)$_2$ (5.3 mg, 24 µmol), triphenylphosphine (19 mg, 72 µmol), K$_2$CO$_3$ (2 g, 14.5 mmol) and freshly distilled 1,4-dioxane were added under nitrogen. The reaction mixture was refluxed for 24 h, and then cooled to RT. The solvent was then evaporated under reduced pressure, and the residue was extracted with water and ethyl acetate (30 ml x 3). The organic layer was washed with brine, dried over MgSO$_4$, filtered and concentrated in vacuo. Purification was accomplished via silica gel column chromatography using hexane:ethyl acetate (5%) as eluent to afford the product as pure solid (60 % yield). ^{1}H NMR (300 MHz, CDCl$_3$): δ 7.984 (s, 2H), 7.50 – 7.47 (d, *J* = 9 Hz, 2H), 7.37 – 7.32 (m, 4H), 7.18 – 7.10 (m, 8H). ^{13}C NMR (75 MHz, CDCl$_3$) δ151.1, 150.9, 146.3, 135.5, 129.7, 127.8, 127.4, 125.8, 124.9, 124.8, 121.3, 115.9. APPI MS (*m/z*): calculated for C$_{25}$H$_{17}$N$_4$ [M + H$^+$]$^+$, 373.1; found, 373.2.

Preparation of {4-[2,6-Bis-(1*H*-tetrazol-5-yl)-pyridin-4-yl]-phenyl}-diphenyl-amine: To a solution of 4-[4-(diphenylamino)phenyl]pyridine-2,6-dicarbonitrile (0.45 g, 1.23 mmol) in DMF (100 mL), sodium azide (0.40 g, 6.16 mmol) and ammonium chloride (0.33 g, 6.15 mmol) were added. The reaction mixture was stirred for 24 h at 125 °C, and then left to cool RT. The inorganic salts were then filtered, and the solvent was removed under reduced pressure. Dilute HCl (0.1 M, 20 ml) was added to yield a suspension that was stirred for 1 h and then refrigerated. The precipitate was filtered, washed with cold water and dried under vacuum to afford the product as a pure solid (94% yield). ^{1}H NMR (300 MHz, DMSO): δ 8.45 (s, 2H), 7.92 – 7.89 (d, 2H, *J* = 8.7 Hz), 7.40 – 7.35 (m, 4H), 7.17 – 7.02 (m, 8H). ^{13}C NMR (75 MHz, DMSO) 156.37,

149.52, 149.23, 146.37, 146.20, 129.80, 128.14, 128.05, 125.17, 124.24, 121.44, 119.32. APPI MS (m/z): calculated for $C_{25}H_{19}N_{10}$ [M + H$^+$]$^+$, 459.2; found, 459.0.

General method for the preparation of the ruthenium complexes T120 and T147: The corresponding ligand (1 eq.), (4,4',4"-trimethoxycarbonyl-2,2':6',2"-terpyridine)RuCl$_3$ (1 eq.) were refluxed overnight under N$_2$ in 5:1:1 ethanol: water: *N*-methylmorpholine. The solvent was then taken off under vacuum and the obtained dark solid was dissolved in water containing excess tetra-butyl ammonium hydroxide (TBAOH), refluxed for 2 h and then applied to a preparative C18-column. The compound was purified by a gradient elution with water/methanol 100%:0% to 80%:20%. Concentrating the solvent containinf the major band under reduced pressure and acidifying to pH 4.2 with 0.1 M HNO$_3$ resulted in a dark precipitate. The solid was filtered to yield a dark solid, which was dried under vacuum at 60 ^{o}C for 24 h. This afforded the two dyes with a TBA$^+$ as a counter cation with quantitative yields.

T120.1TBA: ^{1}H NMR (300 MHz, CDCl$_3$): δ 9.27 (s, 2H), 9.03 (s, 2H), 8,64 (s, 1H), 8.53 (s, 1H), 8.22-8.14 (m, 3H), 7.60 (s, 4H), 7.45-7.40 (m, 5H), 7.23-7.16 (m, 7H), 6.97-6.95 (d, J = 7.8 Hz, 1H), 5.75 (s, 1H). APPI MS (m/z): calculated for $C_{49}H_{29}F_3N_9O_6Ru$ [M -TBA]$^-$, 998.1; found, 998.6.

T147.1TBA: ^{1}H NMR (300 MHz, MeOD): δ 9.21 (s, 2H), 8.93 (s, 2H), 8,80 (s, 2H), 8.07-8.04 (d, 2H, J = 8.7 Hz), 7.58-7.56 (dd, J_1 = 5.7 Hz, J_2 = 1.5 Hz, 2H), 7.46-7.36 (m, 6H), 7.25-7.15 (m, 8H), 3.24 – 3.18 (m, 10H), 1.69 – 1.58 (m, 10H), 1.45 – 1.33 (m, 10H), 1.02 – 0.97 (t, J = 7.2 Hz, 16H). APPI MS (m/z): calculated for $C_{59}H_{61}N_{14}O_6Ru$ [M + TBA - H$^+$]$^-$, 1163.4.1; found, 1163.0.

Preparation of 5,5-bis-(1*H*-tetrazol-5-yl)nonane: To a 100 mL round-bottomed flask, 2,2-dibutylmalononitrile (0.5 g, 2.8 mmol), sodium azide (0.4 g, 6.0 mmol), zinc bromide (1.4 g, 6.0 mmol), 40 ml of water and 40 ml *n*-butanol were added. The reaction mixture was refluxed for 48 h; vigorous stirring is essential. After cooling, the solvent was evaporated under vacuum. HCl (3 N, 60 ml) and ethyl acetate (100 ml) were then added, and vigorous stirring was continued until no solid was present and where the aqueous layer had a pH of 1. If necessary, additional ethyl acetate was added. The organic layer was isolated and the aqueous layer extracted with 2 × 100 ml of ethyl acetate. The combined organic layers were evaporated, 200 ml of 0.25 N NaOH was added, and the mixture was stirred for 30 min, until the original precipitate was dissolved and a suspension of zinc hydroxide was formed. The suspension was filtered, and the solid was washed with 20 ml of 0.25 N NaOH. To the filtrate 40 ml of 3 N HCl was added with vigorous stirring causing the product to precipitate. The product was then filtered and washed with 2 × 20 ml of 3 N HCl and dried in a vacuum-oven to furnish the product as a white powder (92 % yield). ^{1}H NMR (300 MHz, CDCl$_3$): δ 2.27 – 2.22 (m, 4H), 1.21 – 1.16 (m, 4H), 0.91 – 0.88 (m, 4H), 0.79 – 0.75 (t, 6H, J = 7.5 Hz). ^{13}C NMR (75 MHz, CDCl$_3$) 152.8, 59.7, 36.6, 25.5, 22.0, 13.7. APPI MS (m/z): calculated for $C_{11}H_{19}N_8$ [M - H$^+$]$^-$, 263.2; found, 262.9.

Preparation of T162.1TBA: 5,5-Bis-(1*H*-tetrazol-5-yl)nonane (1 eq.), (dcbpy)$_2$RuCl$_2$ (1 eq.) were refluxed overnight under N$_2$ in 5:1:1 ethanol: water: *N*-methylmorpholine. The solvent was then taken off under vacuum and the obtained dark solid was dissolved in water containing excess tetra-butyl ammonium hydroxide (TBAOH) and then applied to a preparative C18-column. The compound was purified by a gradient elution with water/methanol 100%:0% to 80%:20%. Concentrating the solvent that contains the major band under reduced pressure and acidifying to pH 4.2 with 0.1 M HNO$_3$ resulted in a dark precipitate. The solid was and dried under vacuum at 60 $^{\circ}$C for 24 h, affording the dye with one TBA$^+$ as a counter cation with quantitative yields. ^{1}H NMR (500 MHz, MeOD): δ 8.79 – 8.78 (d, *J* = 5.7 Hz, 4H), 7.69 – 7.68 (d, *J* = 6 Hz, 2H), 7.64 (s, 4H), 7.57 – 7.55 (dd, *J$_1$* = 6 Hz, *J$_2$* = 1.5 Hz, 2H), 3.09 – 3.05 (m, 12H), 2.14 – 2.11 (m, 2H), 2.00 – 1.98 (m, 2H), 1.53 – 1.47 (m, 11H), 1.28 – 1.23 (m, 11H), 0.92 – 0.81 (m, 23H), 0.78 – 0.58 (m, 4H), 0.48 – 0.45 (t, *J* = 14.5 Hz, 6H). APPI MS (*m/z*): calculated for C$_{51}$H$_{68}$N$_{13}$O$_8$Ru [M + TBA - H$^+$]$^-$, 1092.3; found, 1092.0.

Results and Discussion

The three ruthenium-based dyes (T120, T147 and T162) were synthesized by stepwise synthetic protocols as shown in Scheme 2. The key steps in the synthesis involve the preparation of the tetrazole-based ancillary ligands.[35] The three dyes were characterized by ^{1}H NMR, UV/Vis, emission and APPI mass spectrometry. The UV/Vis and emission spectra of the three dyes in ethanol are shown in Figure 1 (data is collected in Table 1). The absorption bands between 400 and 800 nm are due to the metal-to-ligand charge transfer bands (MLCT) inferred from TD-DFT calculations, (Scheme S1, Figure S1 and Table S1 in Supporting Information). The emission spectra of the dyes in air-equilibrated ethanol show maxima at 813, 680 and 681 nm when excited at 532 nm for T120, T147 and T162, respectively, Figure 1 and Table 1. The electrochemical properties of the different ruthenium complexes (T120, T147 and T162) were evaluated by differential pulse and cyclic voltammetry in acetonitrile as anchored on a 6 μm titania film. The Ru$^{II/III}$ redox potentials of the three dyes were measured to be $E_{1/2}$ = 0.9, 1.22, and 1.17 V vs NHE for T120, T147 and T162, respectively, Table 1. As expected, T120 had the lowest redox potential due to the effect of the cylometalating trifluoromethylphenyl group. T120 and T147 show, besides the metal's redox peak, an additional redox peak in the scanned potential window that are attributed to the redox active triphenylamine group at ~ 1.25 and 1.30 V vs NHE, respectively. The excited-state oxidation potentials (E_{ox}*) of the dyes, derived from both the redox potential ($E_{1/2}$) and the approximated optical energy gap (E_{0-0}) from the intersection of the corresponding absorption and emission spectra, are more negative than the TiO$_2$ conduction band edge (- 0.7 V vs. NHE),[36] and therefore, upon photo excitation of these complexes electron injection into TiO$_2$ is expected in the order of N719 > T162 > T120 ≈ T147, since T120 and T147 have lower E_{ox}* by ~ 0.09 and 0.16 eV than T162 and N719, respectively.
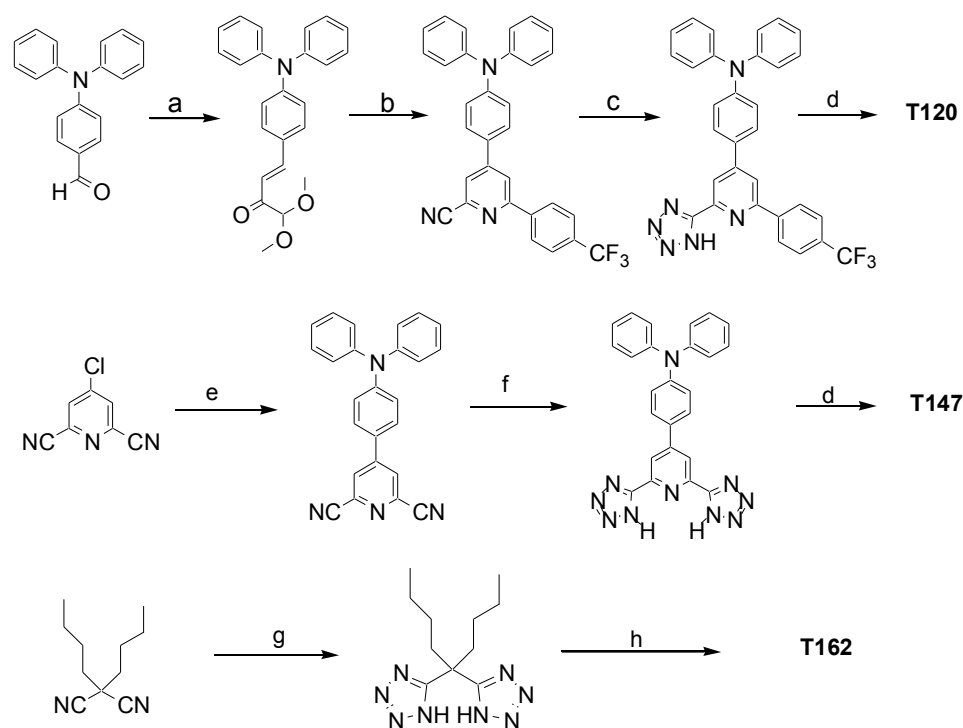
Scheme 2: a) 1,1-dimethoxypropan-2-one, piperidine, methanol, reflux 48 h; **b)** (i) 1-(2-oxo-2-(4-(trifluoromethyl)phenyl)ethyl)pyridinium iodide, NH_4OAc, ethanol, reflux 24 h, (ii) HCl, $CHCl_3$, acetone, reflux 12 h, (iii) NH_2OH, ethanol, reflux 2h, (iv) PPh_3, $(CF_3CO)_2O$, Et_3N, 2h at RT, **c)** NaN_3, NH_4Cl, DMF, 12 h at 120 ^{o}C; **d)** (i) (4,4',4"-trimethoxycarbonyl-2,2':6',2"-terpyridine)$RuCl_3$, ethanol:water:N-methylmorpholine 5:1:1, reflux 24 h, (ii) TBAOH, HNO_3 pH = 4.2; **e)** 4-(diphenylamino)phenylboronic, $Pd(AcO)_2$, PPh_3, K_2CO_3, 1,4-dioxane, reflux for 24 h; **f)** NaN_3, NH_4Cl, DMF, 12 h at 120 ^{o}C; **g)** NaN_3, $ZnBr_2$, butanol:water, reflux for 48 h; **h)** (i) (4,4'-dicarboxybipyridine)$_2RuCl_2$, ethanol:water:N-methylmorpholine 5:1:1, reflux 24 h, (ii) TBAOH, HNO_3 pH = 4.2.

Table 1 Spectroscopic and Electrochemical Data of the Dyes

	λ_{abs}, nm (ϵ, 10^4 M^{-1} cm^{-1})[a]	λ_{em}, nm[b]	$E_{1/2}$, V vs NHE[c]	$E^*_{(ox)}$, V vs NHE	Dye loading (x10^{-8} mol.cm^{-2})[f]
T120	328 (32.68), 424 (2.25), 522 (1.4), 678 (0.22)	813	1.25,[d] 0.90	-0.82	5.68 ± 0.04
T147	330 (3.64), 388 (2.51), 478 (3.37), 602 (0.22)	680	1.30,[d] 1.22	-0.82	6.00 ± 0.03
T162	305 (4.05), 374 (1.27), 512 (1.58)	681	1.17	-0.91	4.72 ± 0.05
N719	306 (4.40), 379 (1.40), 525 (1.35)	755	1.08[e]	-0.98	-

[a] Measured in ethanol. [b] Measured in aerated ethanol with λ_{ex} = 532 nm. [c] Measured as anchored on TiO_2 in acetonitrile with 0.1 M $LiClO_4$. [d] This redox peak is attributed to the triphenylamine moiety. [e] Measured in DMF with 0.1 M $TBAPF_6$. [f] The value was calculated at the MLCT band for the desorbed dye solution from 6μm titania film.
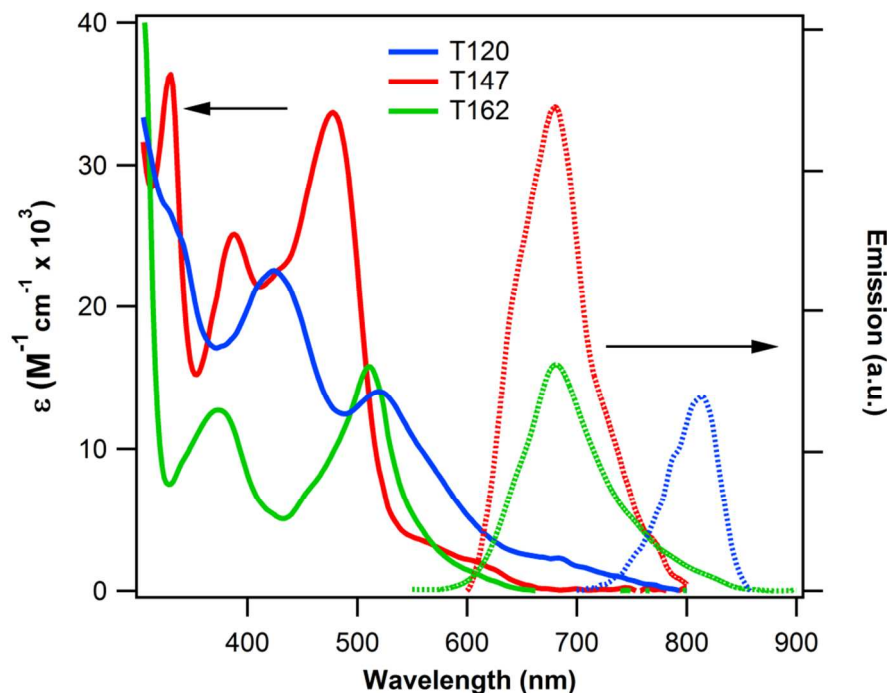
Figure 1: Absorption (solid) and emission (dotted) spectra (λ_{ex} = 532 nm) of T120 (blue), T147 (red) and T162 (green) in ethanol.

DSSCs employing a 14 μm thick TiO_2 layer plus a 6 μm scattering layer (300 nm) were fabricated using the three dyes and N719 for comparison. No co-adsorbent was needed in the case of T162 and T147, however, 20 mM of chenodeoxycholic acid was needed as a de-aggregating agent in the case of T120. An electrolyte solution (EL1) with 1.0 M 1,3-dimethylimidazolium iodide (DMII), 0.1 M guanadinium thiocyanate (GuNCS), 0.1 M LiI, 0.05 M I_2 and 0.5 M 4-*tert*-butylpyridine (TBP), in a mixture of acetonitrile and valeronitrile (85 : 15), was used in these studies. The photocurrent vs voltage (*IV*) responses of the four cells are shown in Figure 2. The T162 based cell afforded the best performance among the three dyes with a short-circuit photocurrent J_{sc} = 12.7 mA.cm^{-2} (10.4 and 11.3 mA.cm^{-2} for T120 and T147, respectively), and open-circuit photovoltage V_{oc} = 685 mV (569 and 685 mV for T120 and T147, respectively), a fill factor *FF* = 0.65 (0.72 and 0.67 for T120 and T147, respectively) and a total efficiency η = 6.0 % (4.3 and 5.3% for T120 and T147, respectively) under a simulated AM1.5 G solar illumination at 100 mW.cm^{-2}. In the case of N719, the cell showed the highest performance with J_{sc} = 15.0 mA.cm^{-2}, V_{oc} = 694 mV, *FF* = 0.67 and η = 7.0 %. The T120 cell showed a strikingly lower voltage than the other three dyes by more than 115 mV that is probably due to accelerated electron recombination processes as suggested by its dark current (Figure 2B). The respective IPCE spectra are shown in Figure 3. As can be seen, the IPCE% of the T162 and N719 maximize between 520 and 530 nm at ~ 84%, which suggests that the injection and collection efficiencies for the T162 cell are similar to that of N719. However, the lower

photocurrent seen for T162 than N719 is mainly due to the blue-shift of the former's absorption in the visible region.
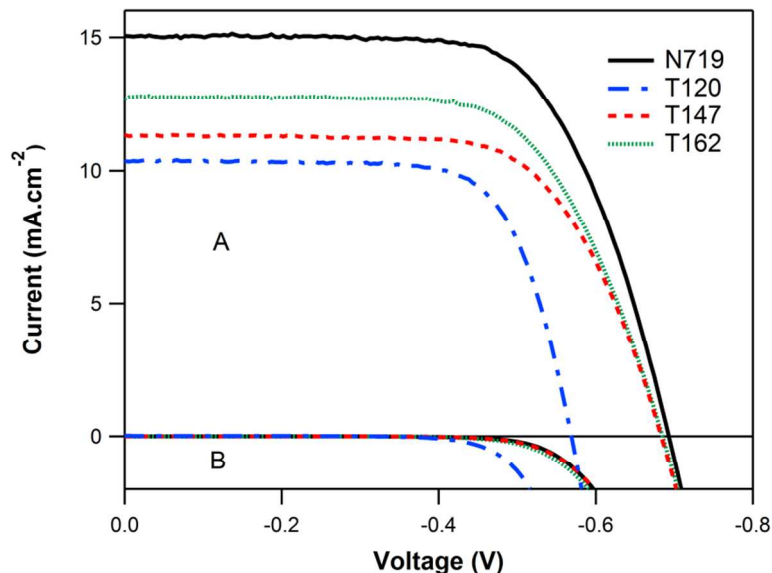

Figure 2: (A) Photocurrent–voltage characteristics of DSSCs sensitized with dyes: N719 (solid – black), T120 (dotted-dashed-blue), T147 (dashed-red) and T162 (dotted -green) assembled with electrolyte EL1. (B) Dark currents of the corresponding cells.

Table 2 DSSCs' Performance of **T120**, **T147**, **T162** and **N719** Dyes

	Electrolyte[a]	J_{sc}, mA.cm^{-2}	V_{oc}, mV	FF	η (%)[b]
T120	EL1	10.4 (10.1[c])	569	0.72	4.3
	EL2	12.6 (12.4[c])	486	0.73	4.5
T147	EL1	11.3 (10.9[c])	685	0.67	5.3
	EL2	13.6 (13.3[c])	635	0.72	6.2
T162	EL1	12.7 (12.3[c])	685	0.65	6.0
	EL2	13.0 (12.7[c])	633	0.72	5.9
N719	EL1	15.0 (14.7[c])	694	0.67	7.0
	EL2	15.3 (15.1[c])	635	0.72	7.0

[a] Electrolyte EL1: 1.0 M DMII, 0.1 M LiI, 0.5 M TBP, 0.1 M GuSCN and 0.05 M I_2 in acetonitrile:valeronitrile (85:15); EL2: 1.0 M DMII, 0.1 M LiI, 0.1 M GuSCN and 0.05 M I_2 in acetonitrile:valeronitrile (85:15). [b] Measured under 100 mW.cm^{-2} simulated AM1.5 spectrum with an active area = 0.126 cm^2. [c] Integrated photocurrent (AM1.5 Global).
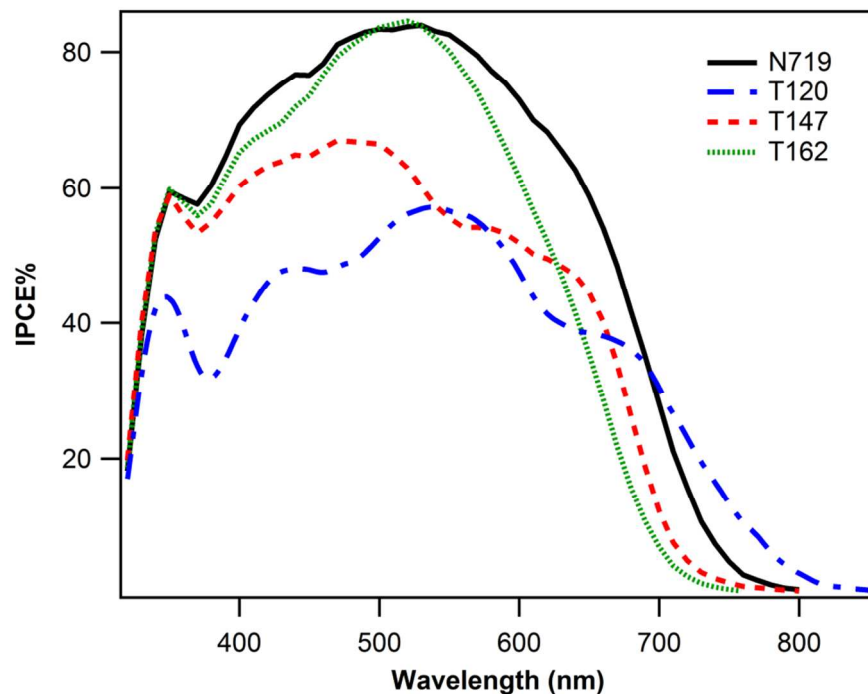
Figure 3: IPCE% and integrated current spectra of N719 (solid – black), T120 (dotted-dashed-blue), T147 (dashed-red) and T162 (dotted -green) DSSC's assembled with electrolyte EL1.

In order to understand the above mentioned results (low performances of T120 and T147), we performed electrochemical impedance spectroscopy (EIS) measurements on the four different assembled cells at V_{oc} under different light intensities. EIS spectra were analyzed using an established equivalent-circuit that interprets the different interfaces in a DSSC through a transmission line model.[37, 38] Figure 4 shows a plot of the chemical capacitance values at the TiO$_2$/electrolyte interface (C_μ), for the different cells extracted from the EIS experiments, versus the applied voltage ($_nE_F - E_{F,redox}$), where $_nE_F$ is the electron quasi-Fermi energy level in the TiO$_2$ film and $E_{F,redox}$ is the electrolyte redox Fermi level. The C_μ values for the four cells show an exponential behavior as a function of the applied voltage, where this is due to the trap energy distribution below the conduction band edge.[39] Considering that the four different cells have the same trap energy distribution (since the TiO$_2$ film is identical in all cells and the same electrolyte solution is used in these cells), the observed shifts in the ($_nE_F - E_{F,redox}$) towards higher or lower values could be attributed to an upward or downward shifts in the conduction band edge, respectively.[40, 41] The observed shift $\Delta(_nE_F - E_{F,redox})$ of T162 compared to N719 lies between -10 and -20 mV, Figure 4. This small shift might be caused in part by the higher number of protons in the case of T162 than N719 (3H's versus 2H's, respectively). As such, we can assume that there is no significant shift in the conduction band edge between the four different cells.
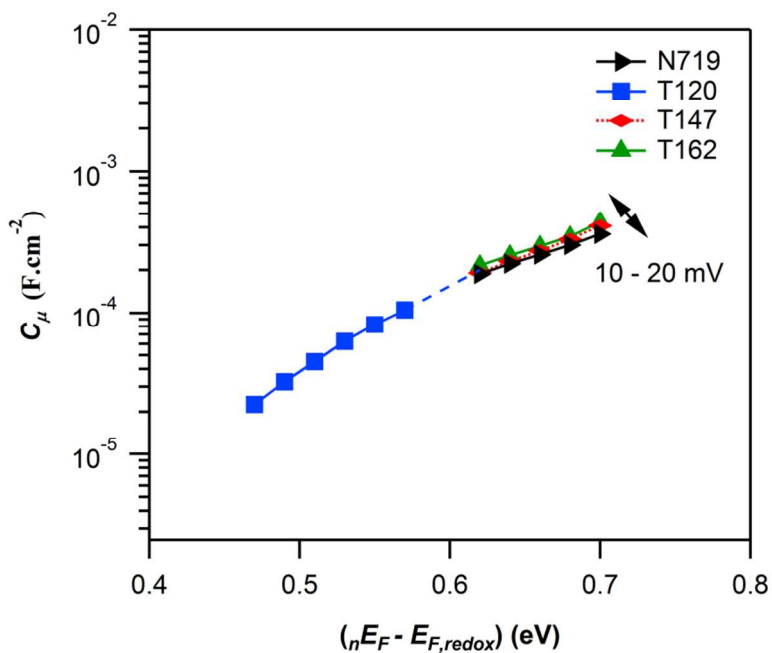
Figure 4: Capacitance values obtained from EIS of N719 (triangle-black), T120 (square-blue), T147 (rhombus -red) and T162 (triangle-green) assembled cells with electrolyte EL1.

Figure 5: Charge transfer resistance values obtained from EIS of N719 (triangle-black), T120 (square-blue), T147 (rhombus-red) and T162 (triangle-green) assembled cells with electrolyte EL1.
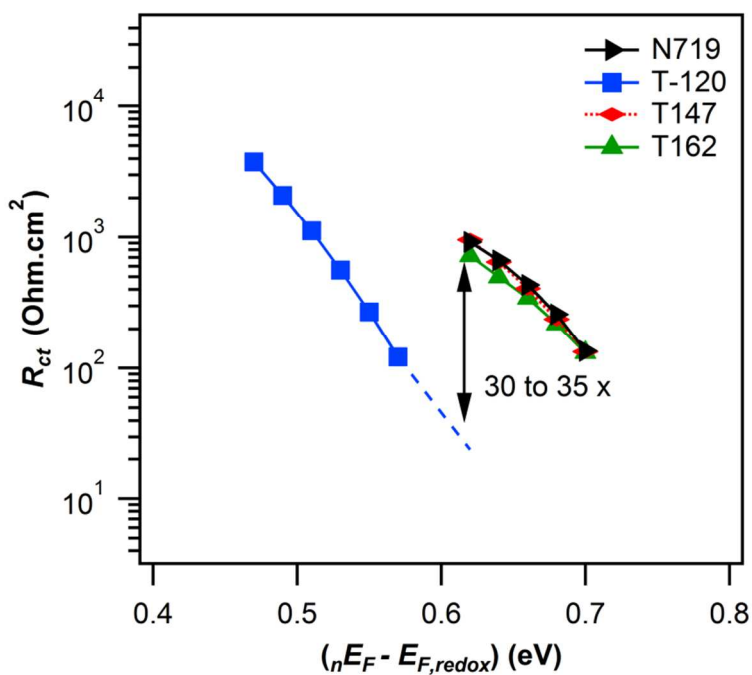
However, the plots of the charge recombination resistance at the TiO_2/electrolyte interface (R_{ct}) versus ($_nE_F - E_{F,redox}$) show profound difference between the T120 and the other three cells, Figure 5. The DSSCs that incorporates T120 shows significantly smaller R_{ct} value by ~ 30 to 35 times. However, the T147 and T162 based DSSC's show similar R_{ct} values to that of N719. These results suggest fast electron recombination processes at the dyed TiO_2/electrolyte interface in the T120 dye case and in turn causes the low V_{oc} value of 569 mV. These results are also consistent with the dark currents measured for the respective cells, Figure 2B. The electron recombination in the T120 based cells can be due to factors such as iodine binding[42] and/or inefficient dye regeneration[43] that would affect negatively the photo-current and photo-voltage and as a consequence the total efficiency. In addition, any aggregation of the T120 dye or lower electron injection than T162 and N719 would also affect the photo-current negatively to a high extent,[44] on a condition that the light harvesting efficiency of T120 would be similar to the other two studied dyes. Indeed, from the LHE% spectra of T120, T147 and T162 dyes when anchored on a 6 μm titania film (Figure S2), one can conclude that the three dyes would absorb more than 99% of the incident light up to 500 nm in the studied and fully assembled cells. As for T147, the following can be deduced from the various data: a- its high redox potential of 1.22 V vs. NHE would ensure its fast regeneration by iodide after electron injection, b- the EIS and dark current spectra suggest slow electron recombination processes, c- its high absorption extinction coefficient and light harvesting efficiency (LHE%), (Figure S2). However, the IPCE spectrum of T147 maximizes to ~ 67% at 470 nm which in turn resulted in its low photocurrent. This made us suspect that T147 does not have high injection efficiency with the electrolyte used (EL1). Indeed, a T147 DSSC incorporating another electrolyte system (EL2) having the same composition as the one described above but lacks the TBP additive, Table 2 and Figure S3, gave higher J_{sc} = 13.6 mA.cm^{-2} and η = 6.2% but a lower V_{oc} = 635 mV as expected when compared to EL1. In addition, a similar effect was seen for T120 which suggested also an inefficient electron injection, where the J_{sc} increased from 10.4 to 12.6 mA.cm^{-2} and the V_{oc} decreased from 569 to 486 mV. No profound effects were seen for T162 and N719 except on the V_{oc}, Table 2. The lack of TBP in the EL2 electrolyte system will result in a positive shift (compared to EL1) in the titania conduction band (E_{CB}) and hence decreasing the V_{oc} and increasing the driving force for electron injection for low lying LUMO dyes. These results are consistent with the estimated $E^*_{(ox)}$ values of the four dyes, Table 1, where the difference in the driving force of electron injection for T120 and T147 when compared to N719 and T162 are ~ -0.16 and -0.09 V, respectively.

In order to test the robustness under light soaking of the three tetrazolate-based dyes, we performed a somehow harsh long-term stability test under one-sun irradiation at 70 °C for 2000 h (the usual testing is done under 1 sun irradiation between 60 and 65 °C for 1000h), Figure 6. DSSCs employing a low volatility electrolyte (EL3) composed of 0.6 M 1,2-dimethyl-3-propylimidazolium iodide (DMPII), 0.5 M N-butylbenzimidazole (NBB), 0.1 M GuNCS, 0.05 M LiI and 0.1 M I_2 in 3-methoxypropionitrile (MPN), were fabricated using the above mentioned three dyes in addition to N719 for comparison.
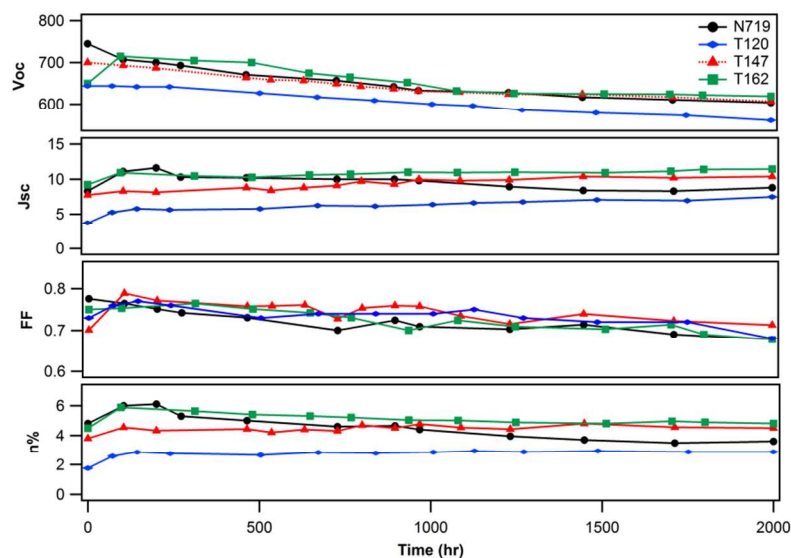
Figure 6: Device performances of N719 (square-black), T120 (rhombus-blue), T147 (triangle - red) and T162 (square-green) assembled cells with the low-volatility electrolyte EL3 under a one-sun light soaking at 70 ^{o}C for 2000 h.

The striking finding from Figure 6 is the fact that the overall efficiencies of the T120 and T147 cells kept relatively constant with time mainly due to the continuous increase in J_{sc} and a concurrent decrease in *FF* and V_{oc} with time. In comparison, the overall efficiencies of the T162 and N719 based cells decreased by ~ 18 and 40%, respectively, after 2000 hours. It's important to note here that the J_{sc} of T162 also increased slightly with time, unlike N719 where the J_{sc} continuously declined with time after the first 100 hours. The main profound changes in the photovoltaic parameters of the four cells were in the *FF* and V_{oc}. It is well know that the E_{CB} of TiO$_2$ shifts positively under light irradiation.[36, 45, 46] The reason behind such shift is yet still not that clear but it might be either due to a change in the surface dipole brought about by an increase in the positive charges (induced by intercalation of protons or lithium cations) at the TiO$_2$ surface and/or a decrease in negative charge[36, 47] or unpinning of the conduction band brought about by the accumulation of holes trapped in surface especially when the titania film is light illuminated especially with UV.[48] It's important to note here that we did not use any UV protection film during light soaking, which in turn may have a profound effect on the positive E_{CB} shifting level due to residual levels of UV light striking the cells from the light source. In addition, UV and thermal stress can cause depletion of the triiodide in the cell, and thus the decrease in V_{oc} can be attributed to a corresponding shift at the electrochemical (Nernst) redox potential of the electrolyte.[49, 50] Therefore, such phenomena would be the reasons behind the decrease in V_{oc} upon light soaking for all of the studied cells. In addition, such a positive shift in the TiO$_2$ conduction band could also increase the electron-injection yield from a low LUMO dye to the TiO$_2$ electrode, such as in the case of T147 and T120. Therefore this could explain the constant increase in the J_{sc} for the T147 and T120 based cell with time, and to a lesser extent that of T162. On the other hand, the decrease in the J_{sc} for N719 based cells upon thermal and light

soaking is attributed by different research groups to the desorption and/or decomposition of the dye especially at the labile SCN⁻site,[51] or even to triiodide loss.[49] Comparing the long-term stability of the two somehow similar dyes T162 and N719, both of which have similar electrochemical, photo-physical and photovoltaic parameters that are due to the similarity in their chemical structures, it would be safe to assume that the weak performance of N719 under prolonged light and thermal stress is due mostly to the presence of the labile SCN⁻ ligands as suggested by some reports in the literature.[5, 6, 51]

Lastly, in order to understand the constant decrease of the *FF* of the four cells, we performed EIS experiments on the fresh and stressed cells. Figure 7 shows the Nyquist plots of a fresh and aged N719 DSSCs. As can be seen, the charge transfer resistance at the Pt/electrolyte interface increased from 2 to 22 $\Omega.cm^2$ in addition to a slight increase in the series resistance (R_s) from 5 to 6.5 $\Omega.cm^2$, suggesting a decrease in activity of the Pt cathode with time. The same phenomenon was seen with all of the aged cells.
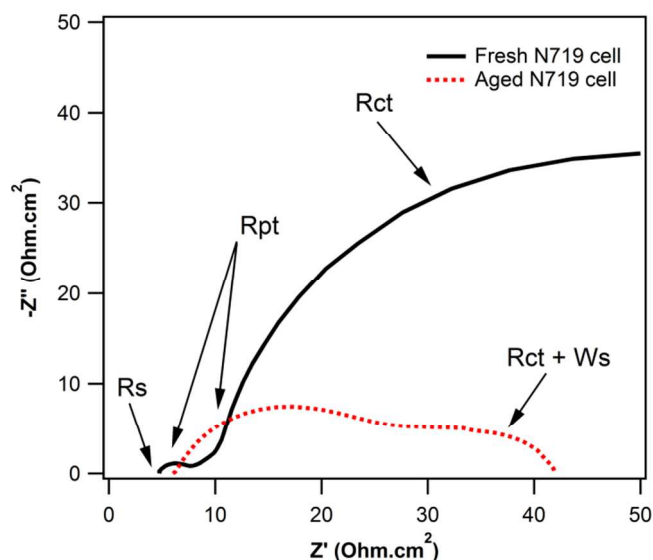

Figure 7: Nyquist plots of a fresh (solid-black) and an aged (dotted-red) N719 DSSCs at V_{oc} assembled with electrolyte EL3.

Many research groups agree on the fact that the loss of Pt activity in an aged DSSC is due to factors such as the dissolution of Pt in the electrolyte system[52-54] and/or adsorption of iodide and iodine on its surface,[55]. Keeping in mind that any dissolution of Pt to Pt^{+2} and/or Pt^{+4} and where these cations can always intercalate and/or adsorb on the titania anode or on the underlying conducting substrate would enhance the electron recombination processes that would affect negatively the V_{oc} in addition to increasing the total DSSC resistance and thus lower *FF*.[52, 56] Indeed, we saw acceleration in the recombination processes (~ 100 times) in all aged cells when compared to the fresh ones as inferred from the plot of R_{ct} versus the applied potential, Figure 8, in addition to a shift in C_μ towards lower values by ~ 50 to 70 mV, Figure 9 (only N719 and

T147 cells are shown for clarity), both of which would cause a decrease in V_{oc}. Therefore, we can safely hypothesize that the low *FF* and V_{oc} values for all cells are mainly due to inherent changes in the TiO$_2$, electrolyte, Pt and/or at their interfaces, and hence the three tetrazolate based dyes show excellent intrinsic stability most probably due to the lack of labile mono-dentate ligands such as the SCN$^-$ in N719.
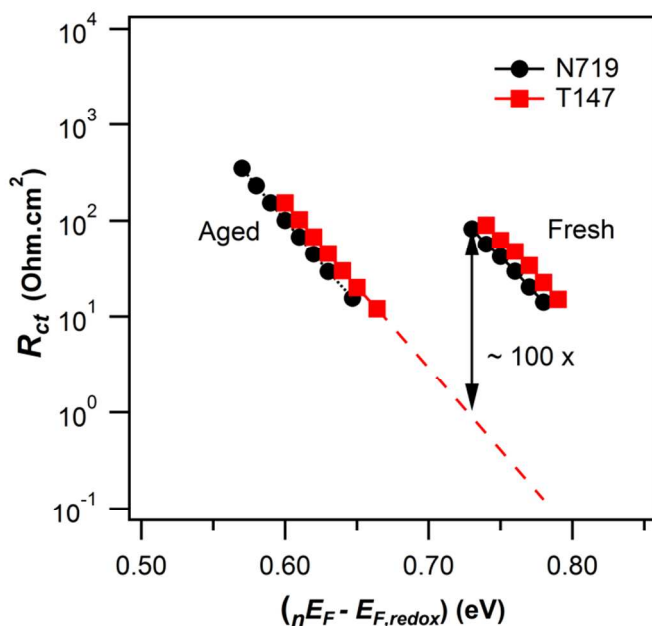

Figure 8: Charge transfer resistance values obtained from EIS of fresh and aged DSSCs of N719 (circle-black) and T147 (square-red) assembled cells with electrolyte EL3.
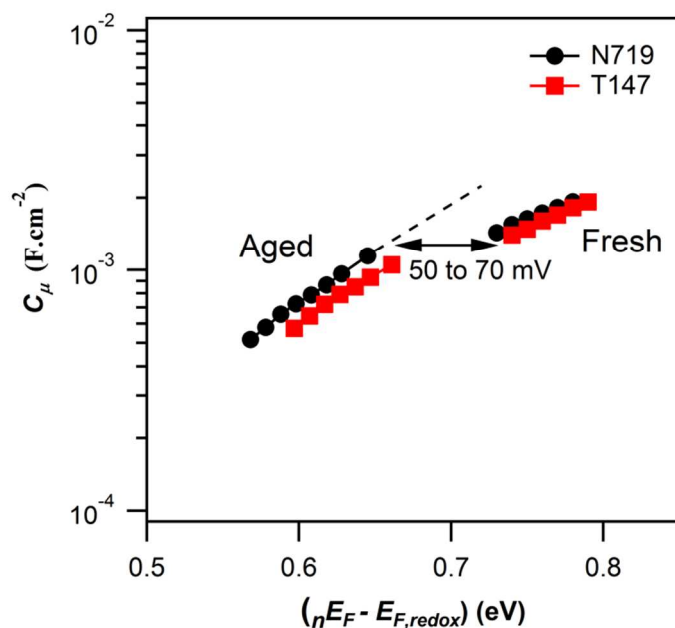
Figure 9: Capacitance values obtained from EIS of fresh and aged DSSCs of N719 (circle-black) and T147 (square-red) assembled cells with electrolyte EL3.

Conclusions

In summary, we have successfully designed and synthesized a new class of ruthenium dyes based on bi- and tri-chelates that contain tetrazolate ligands. The T120 and T147 dyes showed remarkably different efficiencies with different electrolyte compositions. From EIS, electrochemical and photophysical experiments, it was deduced that the above mentioned dyes have relatively lower LUMO levels than N719 and T162. The three new dyes showed striking high stabilities under long-term thermal and light soaking. The robustness of these dyes was attributed to the lack of mono-dentate ligands such as SCN^- as in the case of N719. We are currently designing similar dyes with different substituents selected in a way to increase the absorption extinction coefficient of such dyes and shifting it to lower energies while minimizing aggregation. Such a strategy would hopefully result in highly efficient dyes while maintaining their high stabilities; a crucial pre-requisite for commercialization.

Acknowledgments

References

1. B. O'Regan and M. Grätzel, *Nature*, 1991, **353**, 737-740.
2. A. Yella, H.-W. Lee, H. N. Tsao, C. Yi, A. K. Chandiran, M. K. Nazeeruddin, E. W.-G. Diau, C.-Y. Yeh, S. M. Zakeeruddin and M. Grätzel, *Science*, 2011, **334**, 629-634.
3. S. Mathew, A. Yella, P. Gao, R. Humphry-Baker, F. E. CurchodBasile, N. Ashari-Astani, I. Tavernelli, U. Rothlisberger, K. Nazeeruddin and M. Grätzel, *Nat. Chem.*, 2014, **6**, 242-247.
4. M. K. Nazeeruddin, F. De Angelis, S. Fantacci, A. Selloni, G. Viscardi, P. Liska, S. Ito, B. Takeru and M. Grätzel, *J. Am. Chem. Soc.*, 2005, **127**, 16835-16847.
5. T. Bessho, E. Yoneda, J.-H. Yum, M. Guglielmi, I. Tavernelli, H. Imai, U. Rothlisberger, M. K. Nazeeruddin and M. Grätzel, *J. Am. Chem. Soc.*, 2009, **131**, 5930-5934.
6. M. Grätzel, *Acc. Chem. Res.*, 2009, **42**, 1788-1798.
7. H. T. Nguyen, H. M. Ta and T. Lund, *Sol. Energy Mater. Sol. Cells*, 2007, **91**, 1934-1942.
8. T. A. Shoker and T. H. Ghaddar, *RSC Advances*, 2014, **4**, 18336-18340.
9. T. Funaki, H. Otsuka, N. Onozawa-Komatsuzaki, K. Kasuga, K. Sayama and H. Sugihara, *Inorg. Chem. Commun.*, 2014, **46**, 137-139.
10. C.-Y. Li, C. Su, H.-H. Wang, P. Kumaresan, C.-H. Hsu, I. T. Lee, W.-C. Chang, Y. S. Tingare, T.-Y. Li, C.-F. Lin and W.-R. Li, *Dyes Pigm.*, 2014, **100**, 57-65.
11. C.-H. Siu, C.-L. Ho, J. He, T. Chen, P. Majumda, J. Zhao, H. Li and W.-Y. Wong, *Polyhedron*, 2014, **82**, 71-79.

12.   R. K. Chitumalla, K. S. V. Gupta, C. Malapaka, R. Fallahpour, A. Islam, L. Han, B. Kotamarthi and S. P. Singh, *Phys. Chem. Chem. Phys.*, 2014, **16**, 2630-2640.
13.   S. Sinn, B. Schulze, C. Friebe, D. G. Brown, M. Jäger, J. Kübel, B. Dietzek, C. P. Berlinguette and U. S. Schubert, *Inorg. Chem.*, 2014, **53**, 1637-1645.
14.   Y. Chi, K.-L. Wu and T.-C. Wei, *Chemistry – An Asian Journal*, 2015, 1098–1115.
15.   G. Li, A. Yella, D. G. Brown, S. I. Gorelsky, M. K. Nazeeruddin, M. Grätzel, C. P. Berlinguette and M. Shatruk, *Inorg. Chem.*, 2014, **53**, 5417-5419.
16.   T. Funaki, H. Kusama, N. Onozawa-Komatsuzaki, K. Kasuga, K. Sayama and H. Sugihara, *Eur. J. Inorg. Chem.*, 2014, **2014**, 1303-1311.
17.   D. V. Pogozhev, M. J. Bezdek, P. A. Schauer and C. P. Berlinguette, *Inorg. Chem.*, 2013, **52**, 3001-3006.
18.   H. Kisserwan, A. Kamar, T. Shoker and T. H. Ghaddar, *Dalton Trans.*, 2012, **41**, 10643-10651.
19.   C.-W. Hsu, S.-T. Ho, K.-L. Wu, Y. Chi, S.-H. Liu and P.-T. Chou, *Energy Environ. Sci.*, 2012, **5**, 7549-7554.
20.   C.-C. Chou, K.-L. Wu, Y. Chi, W.-P. Hu, S. J. Yu, G.-H. Lee, C.-L. Lin and P.-T. Chou, *Angew. Chem. Int. Ed.*, 2011, **50**, 2054-2058.
21.   S. Tachiyashiki and K. Mizumachi, *Coord. Chem. Rev.*, 1994, **132**, 113-120.
22.   B. Durham, J. L. Walsh, C. L. Carter and T. J. Meyer, *Inorg. Chem.*, 1980, **19**, 860-865.
23.   R. A. Krause, *Inorg. Chim. Acta*, 1977, **22**, 209-213.
24.   A. Juris, V. Balzani, P. Belser and A. von Zelewsky, *Helv. Chim. Acta*, 1981, **64**, 2175-2182.
25.   M. L. Stone and G. A. Crosby, *Chem. Phys. Lett.*, 1981, **79**, 169-173.
26.   J. K. Son, L. X. Zhao, A. Basnet, P. Thapa, R. Karki, Y. Na, Y. Jahng, T. C. Jeong, B. S. Jeong, C. S. Lee and E. S. Lee, *Eur. J. Medicinal Chem.*, 2008, **43**, 675-682.
27.   F. Qian, J. E. McCusker, Y. Zhang, A. D. Main, M. Chlebowski, M. Kokka and L. McElwee-White, *J. Org. Chem.*, 2002, **67**, 4086-4092.
28.   K.-L. Wu, S.-T. Ho, C.-C. Chou, Y.-C. Chang, H.-A. Pan, Y. Chi and P.-T. Chou, *Angew. Chem. Int. Ed.*, 2012, **51**, 5642-5646.
29.   M. K. Nazeeruddin and M. Grätzel, *Inorg. Syntheses*, 2002, **33**, 185.
30.   M. K. Nazeeruddin, P. Péchy, T. Renouard, S. M. Zakeeruddin, R. Humphry-Baker, P. Cointe, P. Liska, L. Cevey, E. Costa, V. Shklover, L. Spiccia, G. B. Deacon, C. A. Bignozzi and M. Grätzel, *J. Am. Chem. Soc*, 2001, **123**, 1613-1624.
31.   M. J. Frisch and e. al., *Gaussian 03; Gaussian, Inc.: Pittsburgh, PA, 2003.*

32.   P. J. Hay and W. R. Wadt, *J. Phys. Chem.*, 1985, **82**, 270.
33.   M. Cossi and V. Barone, *J. Chem. Phys*, 2001, **115**, 4708-4717.
34.   B. C. O'Regan, J. R. Durrant, P. M. Sommeling and N. J. Bakker, *J. Phys. Chem. C*, 2007, **111**, 14001-14010.
35.   E. S. Andreiadis, R. Demadrille, D. Imbert, J. Pécaut and M. Mazzanti, *Chemistry – A European Journal*, 2009, **15**, 9458-9476.
36.   A. Listorti, C. Creager, P. Sommeling, J. Kroon, E. Palomares, A. Fornelli, B. Breen, P. R. F. Barnes, J. R. Durrant, C. Law and B. O'Regan, *Energy Environ. Sci.*, 2011, **4**, 3494-3501.
37.   Q. Wang, S. Ito, M. Grätzel, F. Fabregat-Santiago, I. n. Mora-Seró, J. Bisquert, T. Bessho and H. Imai, *J. Phys. Chem. B*, 2006, **110**, 25210-25221.
38.   F. Fabregat-Santiago, G. Garcia-Belmonte, I. Mora-Sero and J. Bisquert, *Phys. Chem. Chem. Phys.*, 2011, **13**, 9083-9118.
39.   J. Bisquert, *Phys. Chem. Chem. Phys.*, 2003, **5**, 5360-5364.
40.   V. Gónzalez-Pedro, X. Xu, I. n. Mora-Seró and J. Bisquert, *ACS Nano*, 2010, **4**, 5783-5790.
41.   E. Guillén, L. M. Peter and J. A. Anta, *J. Phys. Chem. C*, 2011, **115**, 22622-22632.

42.   X. Li, A. Reynal, P. Barnes, R. Humphry-Baker, S. M. Zakeeruddin, F. De Angelis and B. C. O'Regan, *Phys. Chem. Chem. Phys.*, 2012, **14**, 15421-15428.

43.   T. Daeneke, A. J. Mozer, T.-H. Kwon, N. W. Duffy, A. B. Holmes, U. Bach and L. Spiccia, *Energy Environ. Sci.*, 2012, **5**, 7090-7099.

44.   H.-P. Lu, C.-Y. Tsai, W.-N. Yen, C.-P. Hsieh, C.-W. Lee, C.-Y. Yeh and E. W.-G. Diau, *J. Phys. Chem. C*, 2009, **113**, 20990-20997.

45.   S. Ferrere and B. A. Gregg, *J. Phys. Chem. B*, 2001, **105**, 7602-7605.

46.   J.-H. Yum, R. Humphry-Baker, S. M. Zakeeruddin, M. K. Nazeeruddin and M. Grätzel, *Nano Today*, 2010, **5**, 91-98.

47.   Q. Wang, Z. Zhang, S. M. Zakeeruddin and M. Grätzel, *J. Phys. Chem. C*, 2008, **112**, 7084-7092.

48.   A. Hagfeldt, U. Björkstén and M. Grätzel, *J. Phys. Chem.*, 1996, **100**, 8045-8048.

49.   A. G. Kontos, T. Stergiopoulos, V. Likodimos, D. Milliken, H. Desilvesto, G. Tulloch and P. Falaras, *J. Phys. Chem. C*, 2013, **117**, 8636-8646.

50.   S. Mastroianni, A. Lanuti, S. Penna, A. Reale, T. M. Brown, A. Di Carlo and F. Decker, *Chemphyschem*, 2012, **13**, 2925-2936.

51.   C. Yoshida, S. Nakajima, Y. Shoji, E. Itoh, K. Momiyama, K. Kanomata and F. Hirose, *J. Electrochem. Soc.*, 2012, **159**, H881-H884.

52.   G. Syrrokostas;, A. Siokoub;, G. Leftheriotis; and P. Yianoulis;, *Sol. Energ. Mater. Sol. C.*, 2012, **103**, 119–127.

53.   G. Wang, Y. Lin, X. Xiao, X. Li and W. Wang, *Surf. Interface Anal.*, 2004, **36**, 1437-1440.

54.   E. Olsen, G. Hagen and S. Eric Lindquist, *Sol. Energy Mater. Sol. Cells*, 2000, **63**, 267-273.

55.   A. T. Hubbard, R. A. Osteryoung and F. C. Anson, *Anal. Chem.*, 1966, **38**, 692-697.

56.   B.-K. Koo, D.-Y. Lee, H.-J. Kim, W.-J. Lee, J.-S. Song and H.-J. Kim, *J. Electroceram.*, 2006, **17**, 79-82.

TOC: We report on a new family of Ru^{II} complexes that bears tetrazolate based ligands with superb long-term stability.

T120   T147   T162